

Discovery, Synthesis, and Structure–Activity Relationship Development of a Series of *N*-4-(2,5-Dioxopyrrolidin-1-yl)phenylpicolinamides (VU0400195, ML182): Characterization of a Novel Positive Allosteric Modulator of the Metabotropic Glutamate Receptor 4 (mGlu₄) with Oral Efficacy in an Antiparkinsonian Animal Model

Carrie K. Jones,^{†,‡,§} Darren W. Engers,^{†,‡,#} Analisa D. Thompson,^{†,‡} Julie R. Field,[†] Anna L. Blobaum,^{†,‡} Stacey R. Lindsley,^{†,‡} Ya Zhou,^{†,‡} Rocco D. Gogliotti,^{†,‡} Satyawan Jadhav,^{†,‡} Rocio Zamorano,^{†,‡} Jim Bogenpohl,[∞] Yoland Smith,[∞] Ryan Morrison,^{†,‡} J. Scott Daniels,^{†,‡} C. David Weaver,^{†,‡} P. Jeffrey Conn,^{†,‡,‡,#} Craig W. Lindsley,^{†,‡,‡,‡,#} Colleen M. Niswender,^{*,†,‡} and Corey R. Hopkins^{*,†,‡,‡,#}

[†]Department of Pharmacology and [‡]Vanderbilt Center for Neuroscience Drug Discovery, Vanderbilt University Medical Center, Nashville, Tennessee 37232, United States

[§]Tennessee Valley Healthcare System, U.S. Department of Veterans Affairs, Nashville, Tennessee 37212, United States

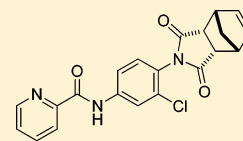
^{||}Department of Chemistry and [⊥]Vanderbilt Institute of Chemical Biology, Vanderbilt University, Nashville, Tennessee 37232, United States

[#]Vanderbilt Specialized Chemistry Center for Accelerated Probe Development (MLPCN), Nashville, Tennessee, 37232, United States

[∞]Yerkes National Primate Research Center and Department of Neurology, Emory University, Atlanta, Georgia 30329, United States

Supporting Information

ABSTRACT: There is an increasing amount of literature data showing the positive effects on pre-clinical antiparkinsonian rodent models with selective positive allosteric modulators of metabotropic glutamate receptor 4 (mGlu₄). However, most of the data generated utilize compounds that have not been optimized for druglike properties, and as a consequence, they exhibit poor pharmacokinetic properties and thus do not cross the blood–brain barrier. Herein, we report on a series of *N*-4-(2,5-dioxopyrrolidin-1-yl)phenylpicolinamides with improved PK properties with excellent potency and selectivity as well as improved brain exposure in rodents. Finally, ML182 was shown to be orally active in the haloperidol induced catalepsy model, a well-established antiparkinsonian model.



15f
hmGlu₄ = 291 ± 55
rmGlu₄ = 376 ± 23
rFS = 11.2 ± 0.8
F = 97%
B/P = 0.93

INTRODUCTION

Parkinson's disease (PD) is a neurodegenerative disease that affects the central nervous system and is present in nearly 1 in 300 adults.¹ With the exception of Alzheimer's disease (AD), PD is the most common neurodegenerative disorder. PD is part of a larger group of conditions known as movement disorders and is characterized by four major primary symptoms: tremor, which is present at rest; bradykinesia, loss of spontaneous movement; rigidity, an increase in muscle tone; and disturbance of posture, an inability to maintain an upright posture.^{1–4} The major motor disturbances in PD patients are due to the loss of mesencephalic dopaminergic neurons in the substantia nigra which results in the decreased stimulation of the motor cortex by the basal ganglia. In addition to the more prominent motor disturbances, PD patients also suffer from significant nonmotor symptoms, such as depression, sleep disorders, and cognitive problems.^{1–6} Although the disease was first noted in the

medical community nearly 200 years ago,⁷ there is still no known cure for PD and, as important, there are very few palliative drugs that provide benefit over the time frame of the disease progression.

Because of the discovery that the loss of dopaminergic neurons is the primary culprit for the motor disturbances in PD patients, the development of dopamine (DA) replacement therapies has dominated the PD treatment landscape.⁸ The primary pharmaceutical used for the treatment of PD is levodopa (L-DOPA), since the use of dopamine itself proved ineffective because it does not cross the blood–brain barrier (BBB). However, it was also discovered that the use of L-DOPA as a stand-alone treatment proved very difficult because of the rapid decarboxylation of L-DOPA that releases vasoactive DA

Received: July 18, 2011

Published: October 3, 2011

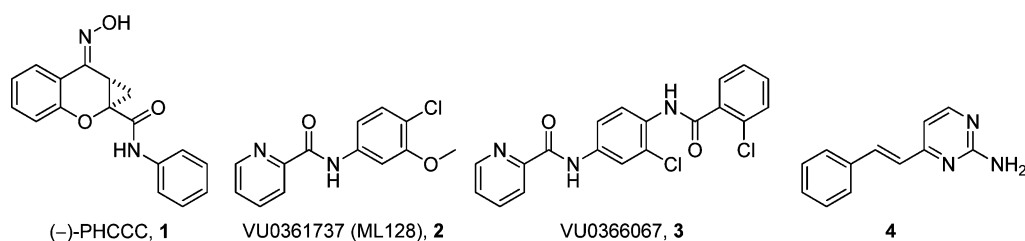


Figure 1. Structures of recently reported mGlu₄ PAMs.

prior to crossing the BBB, resulting in severe cardiovascular events. This side effect can be mitigated by the coadministration of an amino acid decarboxylase inhibitor that significantly increases the levels of DA in the CNS without the cardiovascular side effects.^{3,4} Several other direct-acting DA agonists have been introduced, as well other therapies for increasing DA levels. Although the introduction of L-DOPA has significantly improved the initial treatment of PD, DA-replacement therapies have significant complications with long-term use. For example, a “wearing-off” and “on-off” phenomenon has been noted in which DA-replacement therapies lose efficacy over time, resulting in an ever-increasing dosage cycle.^{9,10} Other consequences of DA-replacement include dyskinesias (rocking movements, repetitive motor behaviors) and psychotic and behavioral disturbances that often develop after long-term usage.¹¹ Because of these significant side effects of DA replacement, alternative approaches toward the treatment and reversal of PD have been investigated, including invasive surgery and deep brain stimulation (DBS), along with attempts to develop agents to manipulate other, potentially druggable targets (e.g., antagonists of A_{2A} adenosine receptors). Because of the limitations of current therapies for PD, we became interested in a potentially new target for the palliative care, and potential disease modification, of PD. Because of exceptionally high expression levels of metabotropic glutamate receptor 4 (mGlu₄) at the striatopallidal synapse of the basal ganglia, we and others have targeted this receptor for therapeutic intervention into PD.^{12–17}

Over the past several years, our laboratories and others have added to the list of selective and novel tool compounds for the study of mGlu₄ via positive allosteric modulation (Figure 1). Thus far, three disclosed mGlu₄ PAMs (2,¹⁸ 3,¹⁹ and 4²⁰) have been shown to be CNS penetrant when dosed systemically, with compounds 2 and 4 exhibiting efficacy in the haloperidol-induced catalepsy assay.^{21,22} In addition to the aforementioned *in vivo* tool compounds, there have been numerous *in vitro* tools reported.^{23–25}

Compound 3 possesses an acceptable balance of *in vitro* pharmacological properties, as well as moderate stability in rat liver microsomes (RLM). While compound 3 was able to cross the blood–brain barrier with an acceptable brain/plasma ratio (*B/P* = 1), its overall brain penetration was substantially reduced compared to the aminopyridine 4. In this study, we disclose a series of *N*-4-(2,5-dioxopyrrolidin-1-yl)phenylpicolinamide mGlu₄ positive allosteric modulators that are CNS penetrant and show oral efficacy in an antiparkinsonian animal model.

RESULTS AND DISCUSSION

Although we have reported on several mGlu₄ *in vitro* and *in vivo* tool compounds, there still remains room for significant improvement in an acceptable probe for the mGlu₄ receptor.

To this end, we started from a functional high-throughput screening (HTS) initiated at Vanderbilt University, TN, and discovered an interesting new lead compound, *N*-(4-(1,1,3,3-tetraoxidobenzo[*d*][1,3,2]dithiazol-2-yl)phenyl)furan-2-carboxamide, 8 (Figure 2, Pubchem compound identification (CID),

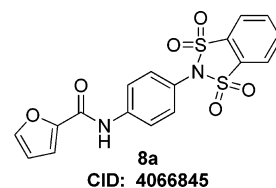
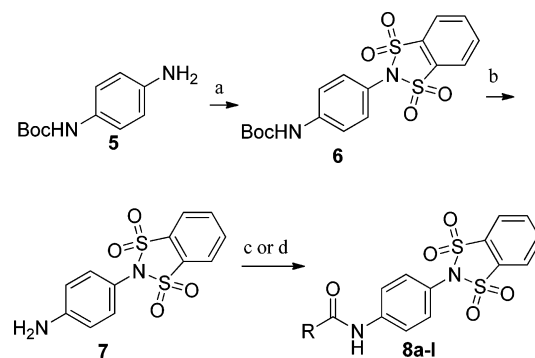


Figure 2. Structure of initial HTS hit.

4066845; ChemDiv ID, K906-0087). Although compound 8 did not possess favorable calculated properties for a CNS probe compound (MW = 404.4, TPSA = 109.9), it represented a submicromolar starting point for our mGlu₄ hit-to-lead program.

The 1,1,3,3-tetraoxidobenzo[*d*][1,3,2]dithiazol-2-yl)phenyl-carboxamide compounds were synthesized as outlined in Scheme 1. Commercially available mono-Boc protected

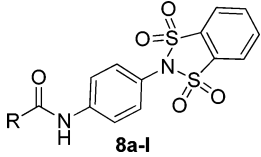
Scheme 1. Synthesis of 1,1,3,3-Tetraoxidobenzo[*d*][1,3,2]-dithiazol-2-yl)phenyl)carboxamides 8a–I^a



^aReagents and conditions: (a) 1,2-benzenedisulfonyl dichloride, Et₃N, CH₂Cl₂; (b) 4.0 M HCl/dioxane, 99% (two steps); (c) RCOCl, CH₂Cl₂, DIEA, 49–87%; (d) RCO₂H, EDCl, HOBT, dioxane/DMF, 27–74%. All library compounds were purified by mass-directed preparative LC with a purity of >95%.

1,4-dianiline 5 was reacted with 1,2-dibenzenedisulfonyl dichloride (Et₃N, CH₂Cl₂), yielding 6. Next, the Boc group was removed under acidic conditions (4.0 M HCl/dioxane), and then the amides 8a–I were formed utilizing either the carboxylic acids (EDCI, HOBT, dioxane/DMF) or acid chlorides (DIEA, CH₂Cl₂).

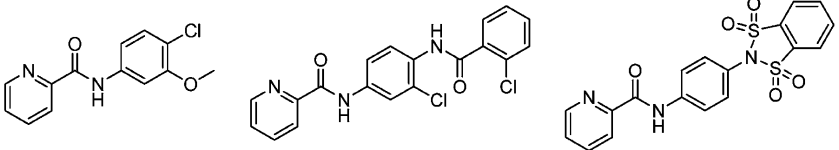
The structure–activity relationship (SAR) surrounding this set of compounds mirrored other series that we have reported previously (Table 1).^{18,19,25} Namely, the 2-pyridylamide 8d was

Table 1. Human mGlu₄ Potency and %GluMax Response (As Normalized to Standard 1) for Selected Western Amide Analogues


compd	R	hEC ₅₀ (nM) ^a	GluMax (% 1) ^a	tPSA	cLogP
8a	2-furan	226 ± 61	110.3 ± 5.8	109.9	1.77
8b	phenyl	402 ± 74	65 ± 1.5	100.6	2.60
8c	cyclohexyl	765 ± 133	48.3 ± 3.3	100.6	3.14
8d	2-pyridyl	136 ± 61	99.7 ± 0.9	113.0	2.19
8e	3-pyridyl	inactive ^b	27.7 ± 2.7	113.0	1.84
8f	4-pyridyl	inactive ^b	22.3 ± 1.9	113.0	1.84
8g	6-fluoro-2-pyridyl	1800 ± 1500	76.7 ± 8.1	113.0	2.42
8h	6-methoxy-2-pyridyl	inactive ^b	22.0 ± 1.2	122.2	2.64
8i	4-pyrimidine	179 ± 36	100.3 ± 4.9	125.3	1.41
8j	2-thiazole	353 ± 125	122.3 ± 5.9	113.0	2.05
8k	4-thiazole	104 ± 34	123 ± 1.2	113.0	2.05
8l	5-thiazole	inactive ^b	39.7 ± 0.3	113.0	2.05

^aEC₅₀ and maximal response when compared to glutamate (GluMax) are the average of at least three independent determinations performed in triplicate (mean ± SEM). **1** is run as a control compound each day, and the maximal response generated in human mGlu₄ CHO cells in the presence of mGlu₄ PAMs varies slightly in each experiment. Therefore, data were further normalized to the relative **1** response obtained in each day's run.

^bInactive compounds are defined as those in which the %GluMax did not surpass 2 × EC₂₀ for that day's run.

Table 2. Characteristics of Previously Reported mGlu₄ Tool Compounds from Vanderbilt University


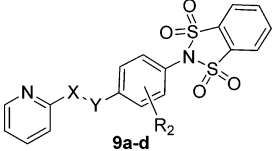
Parameter	2	3	8d
MW	262.7	386.2	414.5
TPSA	50.7	70.6	113.0
cLogP	2.80	2.74	2.19
hmGlu ₄ EC ₅₀ (nM)	240 ± 40	517 ± 57	136 ± 61
rmGlu ₄ EC ₅₀ (nM)	110 ± 30	570 ± 131	165 ± 1
rmGlu ₄ CRC Fold Shift	35.3 ± 2.8	18.3 ± 1.3	5.2 ± 0.6
rat CL _{HEP} (mL/min/kg)	65.5	27.3	ND
rPPB (%fu)	2.4	0.29	3.8
CYP (1A2, 2C9, 3A4, 2D6)	<0.1, >30, >30, >30	>30, 11.8, >30, 13.1	>30
μM			
mGlu selectivity	5.1 μM (5), 2.7 FS (8)	5.3 FS (7), 3.8 FS (8)	selective
B/P	4.1	1.04	0.085

the most potent heterocyclic substituent (hEC₅₀ = 136 nM). Other aryl, cycloalkyl, and five-membered heterocycles also showed submicromolar potency at both the human and rat mGlu₄ receptors. However, despite these modifications, the molecular weight (MW) and polar surface area (TPSA) remained suboptimal for the design of a CNS penetrant probe compound. To confirm this prediction, we profiled **8d** in both in vitro and in vivo rat pharmacokinetic (PK) experiments and assessed the extent of CNS penetration for this compound (Table 2). While the compound displayed selectivity against other mGlu subtypes (mGlu_{1-3,5,6-8}), the extent of brain penetration was poor (B/P = 0.085) following intraperitoneal (ip) administration to rats.

Next we turned our attention to compounds that would have more favorable calculated properties for a CNS penetrant

molecule (MW < 400, TPSA < 90) (Table 3). To this end we examined and evaluated the effect of removing the carbonyl of the amide. Subsequent replacement of the carbonyl with a methylene group (**9b**) or a cyclopropyl group (**9c**) effectively reduced the TPSA (113–96) of the scaffold but with a cost of 10- to 40-fold reduction in mGlu₄ potency. Likewise, the addition of a substituent ortho to the amide on the internal phenyl group (**9a**), or reversing the amide (**9d**), proved to alter the TPSA but again with a significant reduction in the potency for both compounds.

One area of diversification where we have had success with other series is the 4-position of the internal phenyl group. Therefore, we evaluated the activity of a number of substitutions similar to the 1,1,3,3-tetraoxidobenzo[*d*][1,3,2]-dithiazol-2-yl group, in an attempt to reduce TPSA and

Table 3. Human mGlu₄ Potency and Efficacy (As Normalized to Standard 1) for Bis-sulfonamide Scaffold Modifications


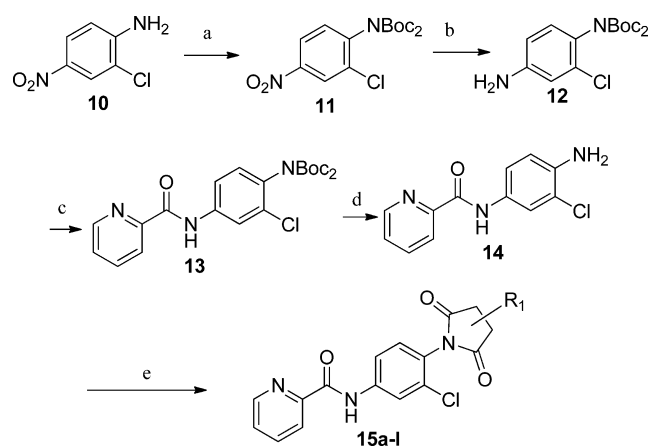
compd	X	Y	R ₂	hEC ₅₀ (nM) ^a	GluMax (% 1) ^a	tPSA	cLogP
9a	CO	NH	2-F	1100 ± 424	67.7 ± 2.7	113	1.89
9b	CH ₂	NH	H	1800 ± 199	110.0 ± 6.2	95.9	1.54
9c	cyclopropyl	NH	H	6400 ± 750	62.7 ± 8.4	95.9	1.88
9d	NH	CO	H	inactive ^b	30.7 ± 2.4	113	2.19

^aEC₅₀ and maximal response when compared to glutamate (GluMax) are the average of at least three independent determinations performed in triplicate (mean ± SEM). 1 is run as a control compound each day, and the maximal response generated in human mGlu₄ CHO cells in the presence of mGlu₄ PAMs varies slightly in each experiment. Therefore, data were further normalized to the relative 1 response obtained in each day's run.

^bInactive compounds are defined as those in which the % GluMax did not surpass 2 × EC₂₀ for that day's run.

ultimately improve brain penetration. The inclusion of an imide group in lieu of the 1,1,3,3-tetraoxidobenzo[*d*][1,3,2]dithiazol-2-yl moiety represented a net lowering of the MW by 60 Da and the TPSA by approximately 30 Å². The synthesis of the imide compounds is shown in Scheme 2.

Scheme 2. Synthesis of *N*-4-(2,5-Dioxopyrrolidin-1-yl)-phenylpicolinamides^a

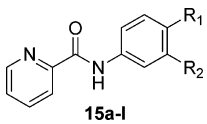


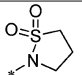
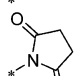
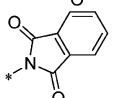
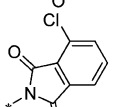
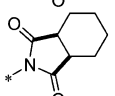
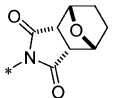
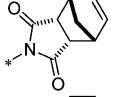
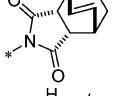
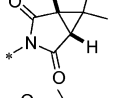
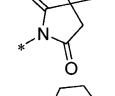
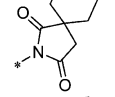
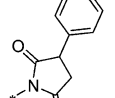
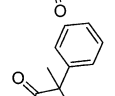
^aReagents and conditions: (a) Boc₂O, DMAP, THF, reflux, 99%; (b) Pd/C, EtOAc, H₂ (1 atm), room temp; (c) picolinoyl chloride HCl, CH₂Cl₂, pyridine, 84%; (d) 4.0 HCl/dioxane; (e) anhydride, toluene/AcOH (3:1), microwave, 150 °C, 90 min. All library compounds were purified by mass-directed preparative LC with purity of >95%.

Evaluation of the compound containing a sultam group revealed a complete loss of activity (16) (Table 4). This core phenyl group does not contain a halogen as do the other compounds; however, the compound containing an internal halogen was not attainable by synthesis. Next, a series of imide compounds were investigated. The initial five-membered imide compound was active (15a, hEC₅₀ = 6200 nM); however, the compound lost ~20-fold activity compared to 8d. Potency could be recovered by increasing the bulk of the right-hand side by utilizing phthalimide (and substituted phthalimides) (15b, hEC₅₀ = 59.4 nM; 15c, hEC₅₀ = 42 nM). However, an initial metabolic stability assessment revealed that these compounds suffered from extensive oxidative metabolism (results not shown). Having demonstrated the phenyl moiety of the phthalimide as the predominant metabolic soft spot, we turned to saturated versions of the phthalimide (15d–i). The initial compound was the direct saturated comparator to 15b

(15d, hEC₅₀ = 370 nM). Although there was a ~10-fold loss of potency, 15d still showed <500 nM potency against hmGlu₄. The trans-isomer was also evaluated with similar potency to the *cis*-15d (results not shown). Increasing the bulk of the saturated six-membered ring resulted in interesting compounds. The [2.2.1]-bridged oxo compound (15e, hEC₅₀ = 1300 nM) exhibited a 4-fold loss in potency; however, the unsaturated [2.2.1]-bridged carbon analogue (15f, hEC₅₀ = 291 nM) and unsaturated [2.2.2]-analogue (15g, hEC₅₀ = 287 nM) were more potent than 15d. Reducing the ring size from six-membered to a substituted three-membered ring resulted in an equipotent compound (15h, hEC₅₀ = 435 nM). Substitution of the five-membered imide led to a loss of activity (15i, hEC₅₀ = 1400 nM), but it remained comparable to the initial five-membered imide (15a). However, when the size of the substituent was increased from the *gem*-dimethyl to cyclohexyl (15j, hEC₅₀ = 158 nM), there was a 10-fold increase in activity. Other bulky substituents were evaluated (15k, hEC₅₀ = 674 nM; 15l, hEC₅₀ = 771 nM); however, these compounds lost activity when compared to 15f.

With our best compounds evaluated for human potency, we evaluated the *in vitro* potency of the compounds on the rat mGlu₄ receptor. Additionally, we compared compounds in terms of their relative efficacy which we evaluated by assessing the ability of a 30 μM concentration of each compound to shift a glutamate concentration–response curve to the left (represented as fold shift, FS) (Table 5). For examination of compound activity at the rat receptor, we employ an assay in which we measure the ability of the G_{i/o}-coupled mGlu₄ receptor to couple to G protein-coupled inwardly rectifying potassium (GIRK) channels.²⁶ In contrast to the calcium mobilization assay, we generally do not observe large increases above the response elicited by saturating concentrations of glutamate alone when GIRK activation is used to assess activity; rather, compounds shift the glutamate concentration–response curve to the left only. Compounds from the 1,1,3,3-tetraoxidobenzo[*d*][1,3,2]dithiazol-2-yl)phenyl)carboxamide series (8d–k) all possessed GluMax values comparable to that of 1, and their efficacies in shifting the glutamate curve were modest, between 3.3 and 7.3. However, moving from the 1,1,3,3-tetraoxidobenzo[*d*][1,3,2]dithiazol-2-yl)phenyl)carboxamide series to the imide series produced significant divergence in compound efficacies. In particular, two phthalimide compounds (15b and 15c) exhibited large differences in efficacy (leftward fold shift values of 23.6 and 83.0, respectively). Compound 15c produced the largest

Table 4. Human mGlu₄ Potency and Efficacy (As Normalized to Standard 1) for Selected Bis-sulfonamide Replacements^a


Cmpd	R ₁	R ₂	hEC ₅₀ (nM)	GluMax (%1)	tPSA	cLogP
16		H	Inactive	25.0 ± 2.5	78.8	1.12
15a		Cl	6200 ± 1700	74.0 ± 4.5	78.8	0.69
15b		Cl	59.4 ± 7.9	103.7 ± 1.2	78.8	3.12
15c		Cl	41.9 ± 5.4	130.3 ± 3.4	78.8	3.86
15d		Cl	370 ± 23	107.0 ± 4.5	78.8	2.12
15e		Cl	1300 ± 180	90.0 ± 1.7	88.1	1.03
15f		Cl	291 ± 55	122.3 ± 1.5	78.8	1.91
15g		Cl	287 ± 62	120.3 ± 5.9	78.8	2.47
15h		Cl	435 ± 118	100.3 ± 2.9	78.8	0.96
15i		Cl	1400 ± 214	82.0 ± 3.5	78.8	1.73
15j		Cl	158 ± 20	78.7 ± 4.2	78.8	2.68
15k		Cl	674 ± 153	116.7 ± 8.3	78.8	2.45
15l		Cl	771 ± 126	123.7 ± 3.5	78.8	2.97

^aEC₅₀ and maximal response when compared to glutamate (GluMax) are the average of at least three independent determinations performed in triplicate (mean ± SEM). **1** is run as a control compound each day, and the maximal response generated in human mGlu₄ CHO cells in the presence of mGlu₄ PAMs varies slightly in each experiment. Therefore, data were further normalized to the relative **1** response obtained in each day's run.

Table 5. Rat mGlu₄ Receptor Potency and Efficacy (Fold Shift) Data for Selected Compounds

compd	EC ₅₀ (nM) ^a	GluMax (% 1) ^a	fold shift
8d	165 ± 1	124.3 ± 3.6	5.2 ± 0.6
8i	242 ± 36	103.3 ± 3.2	3.3 ± 0.3
8j	201 ± 37	127.1 ± 4.5	4.7 ± 0.4
8k	105 ± 15	115.2 ± 2.3	7.3 ± 0.8
15b	66.8 ± 4	131.8 ± 3.9	23.6 ± 3.1
15c	34.9 ± 5.2	137.4 ± 3.2	83.0 ± 16.8
15d	645 ± 63	129.1 ± 2.8	8.3 ± 0.5
15f	376 ± 23	120.3 ± 3.2	11.2 ± 0.8
15g	246 ± 12	122.2 ± 4.5	5.2 ± 1.2
15h	686 ± 32	105.1 ± 0.1	5.5 ± 0.5
15j	397 ± 38	114.2 ± 1.5	4.8 ± 0.2
15k	491 ± 57	137.8 ± 2.0	12.1 ± 1.0
15l	536 ± 105	130.7 ± 3.9	16.7 ± 1.7

^aEC₅₀ and maximal response when compared to glutamate (GluMax) are the average of at least three independent determinations performed in triplicate (mean ± SEM).

leftward shift of the glutamate response curve reported to date. It is also noted that moving away from the phthalimide structures to the saturated imides led to a significant reduction in efficacy and the largest fold shift value for the saturated compounds was 16.7 (**15l**), with most of the compounds tested exhibiting fold shifts of <10 (see Supporting Information Figure 1 for graphs of human and rat potency and fold shift experiments). The exceptions were **15f** (11.2), **15k** (12.1), and **15l** (16.7).

Having identified several key compounds based on human and rat potency as well as efficacy at the rat receptor, we evaluated these compounds in a battery of pharmacokinetic assays including an assessment of intrinsic clearance (CL_{int}) in hepatic microsomes. In addition to intrinsic clearance allowing for the prediction of pertinent rat and human PK parameters (CL and t_{1/2}), intrinsic clearance assessments allow for a rank ordering of compounds with respect to oxidative lability and a subsequent predicted stability in our in vivo PK and efficacy models (Table 6). Although two compounds based on the phthalimide scaffold (**15b** and **15c**) showed excellent in vitro potency on mGlu₄, these compounds have been previously reported by Merck and thus were not further evaluated.²⁷ The three compounds based on the saturated imide scaffold (**15f,j,k**) displayed elevated clearance in human liver microsomes, each predicted to be at hepatic blood flow in humans (Q_H = 21 mL min⁻¹ kg⁻¹). Conversely, an assessment in RLM indicated the compounds to possess moderate-to-high predicted hepatic clearance (CL_{HEP}), with compound **15k** predicting the best stability in rat (CL_{HEP} = 30 mL min⁻¹ kg⁻¹). Assessment of the compound's affinity for plasma proteins was also estimated (amount free and unbound, fu (in %)) in vitro in cryopreserved plasma (Table 6). While compounds **15j** and **15k** were highly protein bound in both human and rat plasma (fu < 1%), **15f** displayed lower protein binding under the same conditions (fu > 3%). In addition, **15f** was also investigated for nonspecific binding (NSB) in freshly prepared rat brain homogenate employing rapid equilibrium dialysis and found to display a decrease in NSB (fu > 7%) relative to binding to plasma proteins. As a first-tier screen for potential drug–drug interaction liability, the compounds were evaluated for their inhibition of the cytochrome P450 (CYP450 or CYP) enzymes utilizing a cocktail approach in human liver microsomes

Table 6. Predicted Hepatic Clearance, Plasma Protein Binding, CYP450 Inhibition, and mGlu Selectivity Values for Selected Compounds

	15f	15j	15k
Intrinsic Clearance ($\text{mL min}^{-1} \text{kg}^{-1}$)			
human CL_{HEP}	19.7	19.4	19.9
rat CL_{HEP}	53.0	66.7	32.6
Plasma Protein Binding (PPB)			
human fu (%)	4.1	0.62	0.02
rat fu (%)	3.2	0.5	0.17
BHB rat fu (%)	7.6	1.7	1.4
CYP450 IC_{50} (μM)			
2C9	>30	>30	8.7
2D6	>30	>30	>30
3A4	>30	>30	>30
2C19	>30	>30	17.6
1A2	>30	>30	8.9
mGlu Selectivity ^a			
mGlu _{1,2,3}	inactive ^b	inactive ^b	inactive ^b
mGlu ₅	PAM, 2.1 FS	inactive ^b	PAM 2.0 FS
mGlu ₆	PAM, 3.1 FS	PAM, 2.1 FS	PAM, 5.8 FS
mGlu ₇	PAM, 2.9 FS	inactive ^b	Ago-PAM, 12.9 FS
mGlu ₈	inactive ^b	inactive ^b	PAM, 2.1 FS

^aSelectivity was assessed by incubating cells with either DMSO-matched vehicle or a 10 μM final concentration of compound in the presence of a full glutamate (or, in the case of mGlu₇, L-AP4) concentration–response curve. FS = fold shift of the glutamate concentration–response curve. Compound 15f showed weak potentiator activity on mGlu₅, mGlu₆, and mGlu₇ (leftward shift of the glutamate concentration–response). ^bInactive compounds showed no ability to left-shift the glutamate response curve at 10 μM . No antagonist activity was noted for any compound at any receptor tested.

designed to inform on the inhibition of the five major drug-metabolizing and/or polymorphic CYPs (CYP2C9, 2D6, 3A4, 2C19, and 1A2). All compounds tested showed no significant activity against CYP2D6 and CYP3A4 (>30 μM), and only 15k showed moderate inhibition of 2C9, 2C19, and 1A2 (8.7, 17.6, and 8.9 μM , respectively).

Lastly, these compounds were evaluated for their selectivity against the other mGlu receptors. For initial studies, 10 μM compound was applied prior to a complete agonist concentration–response curve (CRC) appropriate for each receptor. This technique allows for the detection of potentiator (leftward shift) or antagonist (rightward shift and/or decrease in the maximal response) activity within a single experiment. By use of this assay, all compounds were selective versus the group II mGlu₅ (2 and 3) and only 15f showed weak PAM activity against a group I receptor (mGlu₅, 2.1 FS). However, these compounds did show varying selectivity against the other group III receptors. Whereas 15j only showed weak activity against mGlu₆ (PAM, 2.1 leftward FS of the agonist CRC), 15f was weakly active against both mGlu₆ (PAM, 3.1 FS) and mGlu₇ (PAM, 2.9 FS), and 15k showed activity against all three receptors (mGlu₆, PAM, 5.8 FS; mGlu₇, mixed agonist/PAM (Ago-PAM) activity, 12.9 FS; mGlu₈, PAM, 2.1 FS); the allosteric agonist activity against mGlu₇ was equivalent to that observed for mGlu₄ (12.9 FS vs 12.1 FS).

The predicted in vitro ADME properties of these compounds were consistent with advancement for in vivo studies. Thus, the hydrochlorides of these compounds (15f, 15j, 15k) were synthesized and dosed intravenously (1 mg/kg) and orally (10 mg/kg) to determine pertinent PK parameters such as

clearance (CL), volume of distribution at steady state (V_{ss}), half-life ($t_{1/2}$), and bioavailability (F) (Table 7). Although

Table 7. Rat in Vivo Pharmacokinetic Values for Selected Compounds

PK parameter (rat)	15f	15j	15k
iv (1 mg/kg) ^a			
CL ($\text{mL min}^{-1} \text{kg}^{-1}$)	36.9	48.3	5.4
$t_{1/2}$ (min)	40.4	93.8	329
MRT	493	57.2	109
V_{ss} (L/kg)	18	5.5	0.58
AUC_{0-24} (ng·h/mL)	454	346	3225
po dose (10 mg/kg) ^b			
AUC_{0-24} (h·ng/mL)	4354	813	2685
C_{max} (ng/mL)	238	18.3	553
T_{max} (h)	0.62	7	0.5
F (%)	97	24.6	8.3

^a10% EtOH, 80% PEG-400, 10% saline. ^b10% Tween 80 in 0.5% methylcellulose.

all three compounds displayed modest stability (CL_{HEP}) when assessed in rat liver microsomes, 15k proved to be a lower clearance compound in vivo ($5.4 \text{ mL min}^{-1} \text{kg}^{-1}$). Both 15f and 15j demonstrated moderate clearance values (37 and $48 \text{ mL min}^{-1} \text{kg}^{-1}$, respectively), values that correlated well with their in vitro CL_{HEP} values. Because of the exceptional stability of 15k following intravenous administration to the rat, we evaluated this compound in both beagle dog and rhesus monkey employing an iv cassette dosing paradigm. Compound 15k showed excellent stability in both dogs (CL , $7 \text{ mL min}^{-1} \text{kg}^{-1}$) and monkeys ($3 \text{ mL min}^{-1} \text{kg}^{-1}$) with each species displaying a $t_{1/2}$ of ≥ 3 h. Although 15k showed superior stability comparatively, it unfortunately displayed an oral bioavailability of less than 10%. Conversely, compound 15f demonstrated an excellent oral bioavailability of 97%, whereas 15j displayed a modest bioavailability of 25%.

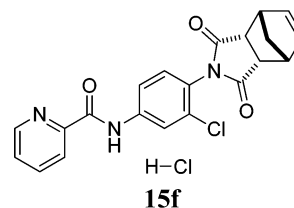
The combination of enhanced bioavailability, oral PK, and an exceptionally low protein binding value indicated that compound 15f possessed the characteristics to be a potential tool compound that could be evaluated for brain exposure after oral dosing (Table 8). The hydrochloride salt of 15f was dosed

Table 8. PO Pharmacokinetic Parameters of 15f (10 mg/kg, 10% Tween 80 in 0.5% Methylcellulose)

PK parameter	
systemic, AUC, 0–6 h ^a (nM·h)	8.58
HPV, AUC, 0–6 h ^a (nM·h)	8.48
brain, AUC, 0–6 h ^a (nM·h)	800
$\text{AUC}_{\text{brain}}/\text{AUC}_{\text{sys}}$	0.93
$\text{AUC}_{\text{sys}}/\text{AUC}_{\text{HPV}}$	1.01

^apo dose, vehicle: 10 mg/kg, 10% Tween 80 in 0.5% methylcellulose.

orally in a microsuspension (10% Tween-80 in 0.5% methylcellulose), and plasma (systemic and hepatic portal) and brain samples were collected for bioanalysis of parent compound up



to 6 h following administration of the compound. The compound showed similar levels in the systemic and HPV plasma, indicating negligible hepatic first pass metabolism ($AUC_{\text{sys}}/AUC_{\text{HPV}} = 1.01$). Compound **15f** also displayed exceptional CNS penetration, with compound exposures reaching 800 nM·h (AUC_{0-6}) and a corresponding brain/plasma ratio that reached unity (0.93).

Considering the promising PK results for **15f**, we evaluated the compound for selectivity against the other mGlu subtypes. In these studies, a 10-point concentration–response of **15f** was applied prior to an EC_{20} concentration of agonist appropriate for each receptor. As with our original fold shift-type studies, **15f** was shown to be inactive against mGlu_{1,2,3,8} and was active against mGlu₅ (PAM, $EC_{50} = 1.7 \pm 0.8 \mu\text{M}$, $64.3 \pm 0.8\%$ GluMax), mGlu₆ (PAM, $EC_{50} > 10 \mu\text{M}$, $45.8 \pm 3.0\%$ GluMax), and mGlu₇ (PAM, $2.9 \pm 0.7 \mu\text{M}$, $64.0 \pm 1.4\%$ GluMax) (see Supporting Information Table 1). In addition, **15f** was tested in Ricerca's lead profiling screen (binding assay panel of 68 GPCRs, ion channels and transporters screened at 10 μM) and was found to be not significant with all the 68 assays conducted (no inhibition of radioligand binding, >50% at 10 μM).

On the basis of the previous PK studies, **15f** was chosen as a potential tool compound for an in vivo proof-of-concept study and was examined in a rat model of neuroleptic-induced catalepsy. Here we evaluated the ability of **15f** to reverse haloperidol-induced catalepsy, a preclinical rodent model of motor impairments associated with Parkinson's disease. The D₂ receptor antagonist haloperidol induced robust catalepsy (Figure 3). As shown in Figure 3, **15f** (0.1–56.6 mg/kg, po)

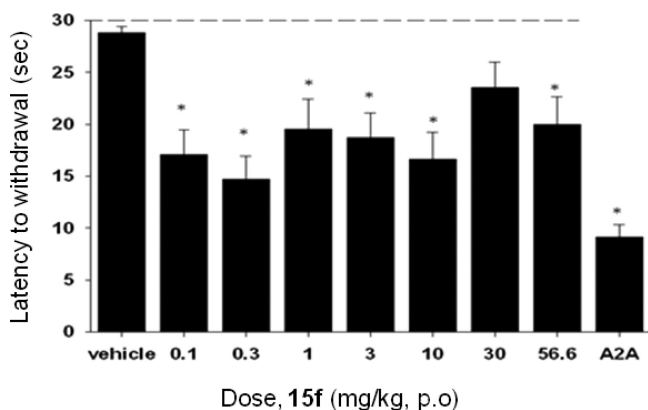


Figure 3. Reversal of haloperidol-induced catalepsy in rats by **15f** after oral dosing. Catalepsy was measured in haloperidol treated (0.75 mg/kg) rats after oral administration of compound (0.1, 0.3, 1, 3, 10, 30, and 56.6 mg/kg) after 30 min. An adenosine A_{2A} antagonist from Neurocrine Biosciences²⁸ was used as a positive control at 56.6 mg/kg, po.

produced a reversal of haloperidol-induced catalepsy ($F_{(8,89)} = 5.8697$, $p < 0.0001$), significant at doses of 0.1–56.6 mg/kg, compared with the vehicle control. The effects of **15f** were equally efficacious compared to those observed using an adenosine A_{2A} antagonist from Neurocrine Bioscience (compound **23**)²⁸ as a positive control, administered at a dose of 56.6 mg/kg, po.

CONCLUSION

We have discovered and characterized a new mGlu₄ PAM in vivo tool compound with activity in a preclinical model of Parkinson's

disease. This new class of *N*-4-(2,5-dioxopyrrolidin-1-yl)-phenylpicolinamides (such as **15f**, VU0400195 (ML182))²⁹ was discovered utilizing a rational drug design approach based on the 1,1,3,3-tetraoxidobenzo[*d*][1,3,2]dithiazol-2-yl)phenyl)-carboxamides (**8d**) scaffold that possessed suboptimal properties. A common feature in many of the reported mGlu₄ PAMs is the presence of a picolinamide moiety which this new scaffold also possesses. However, these new compounds are structurally distinct from previously reported structures because of the presence of the 2,5-dioxopyrrolidin-1-yl moiety. The present report represents only the second example of a potent and selective, orally active mGlu₄ PAM.²⁰

EXPERIMENTAL SECTION

General. All NMR spectra were recorded on a 400 MHz AMX Bruker NMR spectrometer. ¹H chemical shifts are reported in δ values in ppm downfield with the deuterated solvent as the internal standard. Data are reported as follows: chemical shift, multiplicity (s = singlet, d = doublet, t = triplet, q = quartet, br = broad, m = multiplet), integration, coupling constant (Hz). Low resolution mass spectra were obtained on an Agilent 1200 series 6130 mass spectrometer with electrospray ionization. High resolution mass spectra were recorded on a Waters Q-TOF API-US plus Acquity system with electrospray ionization. Analytical thin layer chromatography was performed on EM reagent 0.25 mm silica gel 60-F plates. All samples were of $\geq 95\%$ purity as analyzed by LC–UV/vis-MS. Analytical HPLC was performed on an Agilent 1200 series with UV detection at 214 and 254 nm along with ELSD detection. LC/MS parameters were as follows: method 1 = (J-Sphere80-C18, 3.0 mm \times 50 mm, 4.1 min gradient, 5% [0.05% TFA/CH₃CN]/95% [0.05%TFA/H₂O] to 100% [0.05%TFA/CH₃CN]; method 2 = (Phenomenex-C18, 2.1 mm \times 30 mm, 2 min gradient, 7% [0.1%TFA/CH₃CN]/93% [0.1%TFA/H₂O] to 100% [0.1%TFA/CH₃CN]; method 3 = (Phenomenex-C18, 2.1 mm \times 30 mm, 1 min gradient, 7% [0.1%TFA/CH₃CN]/93% [0.1%TFA/H₂O] to 95% [0.1%TFA/CH₃CN]. Preparative purification was performed on a custom HP1100 purification system¹⁶ with collection triggered by mass detection. Solvents for extraction, washing, and chromatography were HPLC grade. All reagents were purchased from Aldrich Chemical Co. and were used without purification.

tert-Butyl (4-(1,1,3,3-Tetraoxidobenzo[*d*][1,3,2]dithiazol-2-yl)phenyl)carbamate (6). A solution of *N*-Boc-*p*-phenylenediamine **5** (0.68 g, 3.26 mmol, 1.0 equiv) and Et₃N (0.51 mL, 7.19 mmol, 2.2 equiv) in dry DCM (29 mL) was added via syringe pump (8 mL/h) to a refluxing solution of 1,2-benzenedisulfonyl dichloride (0.90 g, 3.27 mmol, 1.005 equiv) in DCM (135 mL). After the complete addition, the solution was maintained at reflux for an additional 2 h. The heat was removed, and after 16 h at room temperature, the solvent was removed under reduced pressure. The residue of the crude reaction mixture was redissolved in DCM (75 mL), washed with saturated NaHCO₃ (aqueous, 75 mL), brine (75 mL), and dried (MgSO₄). After the filtration and concentration under reduced pressure, analytical LCMS confirmed the product (**6**). The material was taken through to the deprotection step. ¹H NMR (400 MHz, CDCl₃): δ 8.11–8.08 (m, 2 H), 7.99–7.96 (m, 2 H), 7.59–7.55 (m, 4 H), 6.66 (br s, 1 H), 1.54 (s, 9 H).

2-(4-Aminophenyl)benzo[*d*][1,3,2]dithiazole 1,1,3,3-Tetraoxide (7). To a solution of **6** (3.26 mmol, 1.0 equiv) in DCM (100 mL) at 0 °C was added dropwise 4 N HCl in dioxane (20 mL). After 15 min, the ice bath was removed. Once the starting material was no longer evident by TLC, the solvent was removed affording the HCl salt (**7**), which was taken through to the amide formation step. LCMS: $t_R = 3.319$ min, $m/z = 311.0$ [M + H]⁺. ¹H NMR (400 MHz, DMSO-*d*₆) δ 8.55–8.51 (m, 2 H), 8.21–8.17 (m, 2 H), 7.17–7.15 (m, 2 H), 6.75–6.73 (m, 2 H).

***N*-(4-(1,1,3,3-Tetraoxidobenzo[*d*][1,3,2]dithiazol-2-yl)phenyl)picolinamide (8d).** To a solution of the HCl salt (**7**) (1.0 equiv) in DCM/DIEA (4:1) (1 mL, 0.1 M) was added picolinyl acid chloride (1.0 equiv). After 12 h at room temperature, the desired

analogue **8d** was obtained as a tan solid (49%). Analytical LCMS: $t_R = 3.074$ min, >98% (214 nm), $m/z = 416.1$ $[M + H]^+$; 1H NMR (400 MHz, DMSO- d_6) δ 11.08 (br s, 1 H), 8.79 (d, 1 H, $J = 4.0$ Hz), 8.60–8.59 (m, 2 H), 8.24–8.21 (m, 5 H), 8.11 (t, 1 H, $J = 8.0$ Hz), 7.73 (t, 1 H, $J = 4.8$ Hz), 7.59 (d, 2 H, $J = 8.4$ Hz); ^{13}C NMR (125 MHz, DMSO- d_6) δ 163.5, 149.8, 148.9, 142.1, 138.7, 136.8, 134.0, 133.0, 127.7, 123.8, 123.1, 122.4, 119.1. HRMS calcd for $C_{18}H_{13}N_3O_5NaS_2$ $[M + Na]^+$, 438.0194; found 438.0194.

Bis(tert-butyl-2-chloro-4-nitrophenyl)carbamate (11). To a solution of 2-chloro-4-nitroaniline **10** (5.0 g, 29 mmol) and DMAP (50 mg, 0.41 mmol) in dry THF (250 mL) was added Boc_2O (16.0 g, 73.3 mmol). The mixture was heated to reflux. After 1 h, the solvent was removed. The residue was redissolved in EtOAc/0.5 N HCl (aqueous), and the organic layer was separated. The aqueous layer was extracted with EtOAc (3 \times 50 mL), and the collected organic layers were washed with brine (100 mL). The solution was dried ($MgSO_4$), filtered, and concentrated to afford bis(tert-butyl-2-chloro-4-nitrophenyl)carbamate **11**. LCMS: $t_R = 3.74$ min, >98% at 254 nM, $m/z = 767.2$ $[2M + Na]^+$.

Bis(tert-butyl-4-amino-2-chlorophenyl)carbamate (12). To a solution of bis(tert-butyl-2-chloro-4-nitrophenyl)carbamate **11** (29.0 mmol) in EtOAc (120 mL) was added 5% Pd/C (150 mg), and an H_2 atmosphere was applied. After 12 h, TLC confirmed loss of starting material. The reaction mixture was filtered through Celite and concentrated to afford bis(tert-butyl-4-amino-2-chlorophenyl)carbamate which was used without further purification. 1H NMR (400 MHz, $CDCl_3$) δ 6.94 (d, 1 H, $J = 8.4$ Hz), 6.72 (d, 1 H, $J = 2.8$ Hz), 6.53 (dd, 1 H, $J = 8.4, 2.8$ Hz), 3.75 (br s, 2 H), 1.41 (s, 18 H).

Bis(tert-butyl-2-chloro-4-(picolinamido)phenyl)carbamate (13). A solution of bis(tert-butyl-4-amino-2-chlorophenyl)carbamate **12** (29.0 mmol) in DCM (25 mL) at 0 °C was subjected to DIEA (10.2 mL, 72.5 mmol) followed by picolinoyl chloride hydrochloride (5.68 g, 31.9 mmol). After 12 h, the mixture was added to EtOAc/ H_2O (1:1, 120 mL). The organic layer was washed with water (2 \times 50 mL), brine (50 mL) and dried ($MgSO_4$). The mixture was filtered and concentrated to provide bis(tert-butyl-2-chloro-4-(picolinamido)phenyl)carbamate **13**. 1H NMR (400 MHz, $CDCl_3$) δ 10.17 (br s, 1 H), 8.63 (d, 1 H, $J = 4.0$ Hz), 8.32 (d, 1 H, $J = 8.0$), 8.05 (d, 1 H, $J = 2.4$ Hz), 7.96 (ddd, 1 H, $J = 8.0, 8.0, 1.2$), 7.66 (dd, 1 H, $J = 8.4, 2.4$), 7.55–7.52 (m, 1 H), 7.20 (d, 1 H, $J = 8.8$ Hz), 1.40 (s, 18 H).

N-(4-Amino-3-chlorophenyl)picolinamide (14). To a solution of bis(tert-butyl-2-chloro-4-(picolinamido)phenyl)carbamate **13** (29.0 mmol) in DCM (300 mL) at 0 °C was added dropwise 4 N HCl in dioxane (50 mL). After 15 min, the ice bath was removed. Once the starting material was no longer evident by TLC, the solvent was removed, affording the HCl salt. The crude material was redissolved with EtOAc (100 mL) and washed with $NaHCO_3$ (aqueous). The organic layer was dried ($MgSO_4$), filtered, and concentrated to afford *N*-(4-amino-3-chlorophenyl)picolinamide **14**. LCMS: $t_R = 1.15$ min, >98% at 254 nM, $m/z = 248.0$ $[M + H]^+$.

General Cyclic Imide Formation. To a solution of *N*-(4-amino-3-chlorophenyl)picolinamide **14** (1.0 equiv) in toluene/acetic acid (3:1) was added the desired anhydride (1.25 equiv), and the mixture was heated to 150 °C in the microwave for 90 min. After LCMS confirmed the product, the mixture was added to EtOAc/ $NaHCO_3$ (saturated) (1:1). The organic layer was separated, washed with brine, and dried ($MgSO_4$). After the organic layer was filtered and concentrated, the material was purified by LC (Gilson) or crystallization.

N-(3-Chloro-4-((1R,2S,3R,4S)-bicyclo[2.2.1]hept-5-ene-1,3-dioxo-1H-isoindol-1-yl)phenyl)picolinamide (15f). Following the general procedure, *N*-(3-chloro-4-((1R,2S,3R,4S)-bicyclo[2.2.1]hept-5-ene-1,3-dioxo-1H-isoindol-1-yl)phenyl)picolinamide was obtained (mixture of diastereomers). LCMS: $t_R = 1.367$ min, >98% at 254 nM, $m/z = 394.0$ $[M + H]^+$. 1H NMR (400 MHz, MeOD) δ 8.81 (d, 1 H, $J = 4.4$ Hz), 8.40 (s, 1 H), 8.31–8.28 (m, 1 H), 8.20 (d, 1 H, $J = 2.4$ Hz), 7.84 (m, 1 H), 7.79 (d, 1 H, $J = 2.4$ Hz), 7.05 (d, 1 H, $J = 8.4$ Hz), 6.31 (s, 2 H), 3.61–3.56 (m, 2 H), 3.44–3.42 (m, 2 H), 1.79–1.76 (m, 1 H), 1.71–1.68 (m, 1 H); ^{13}C NMR (125 MHz, DMSO- d_6 , mixture of diastereomers) δ 176.5, 176.4, 163.44, 163.42, 149.8, 149.7, 148.9, 140.7, 140.4, 138.7, 135.3, 135.0, 131.7, 131.2,

130.6, 127.7, 126.0, 125.6, 123.1, 121.34, 121.31, 120.2, 119.9, 52.4, 52.1, 46.9, 45.7, 45.3, 44.9. HRMS calcd for $C_{21}H_{17}N_3O_3Cl$ $[M + H]^+$, 394.0958; found 394.0959.

N-(3-Chloro-4-(1,3-dioxo-2-azaspiro[4.5]decan-2-yl)phenyl)picolinamide (15j). Following the general procedure, *N*-(3-chloro-4-(1,3-dioxo-2-azaspiro[4.5]decan-2-yl)phenyl)picolinamide was obtained. LCMS: $t_R = 1.439$ min, >98% at 254 nM, $m/z = 398.2$ $[M + H]^+$. 1H NMR (400 MHz, DMSO- d_6) δ 11.01 (br s, 1 H), 8.76 (d, 1 H, $J = 4.4$ Hz), 8.24 (d, 1 H, $J = 2.0$ Hz), 8.17 (d, 1 H, $J = 8.0$ Hz), 8.08 (ddd, 1 H, $J = 8.0, 8.0, 2.0$ Hz), 7.99 (dd, 1 H, $J = 8.4, 2.0$ Hz), 7.70 (ddd, 1 H, $J = 7.6, 4.8, 1.2$ Hz), 7.39 (d, 1 H, $J = 8.4$ Hz), 2.86 (d, 1 H, $J = 18.0$ Hz), 2.78 (d, 1 H, $J = 18.4$ Hz), 1.77–1.60 (m, 7 H), 1.46–1.24 (m, 3 H); ^{13}C NMR (125 MHz, DMSO- d_6) δ 181.6, 175.1, 163.4, 149.7, 148.9, 140.7, 138.7, 131.7, 131.7, 131.1, 127.7, 125.8, 123.1, 121.3, 120.1, 45.3, 39.3, 34.0, 32.5, 25.1, 22.0, 21.9. HRMS calcd for $C_{21}H_{21}N_3O_3Cl$ $[M + H]^+$, 398.1271; found 398.1271.

N-(3-Chloro-4-(2,5-dioxo-3-phenylpyrrolidin-1-yl)phenyl)picolinamide (15k). Following the general procedure, *N*-(3-chloro-4-(2,5-dioxo-3-phenylpyrrolidin-1-yl)phenyl)picolinamide was obtained as a mixture of diastereomers (dr 2:1). Major diastereomer, LCMS: $t_R = 1.370$ min, >98% at 254 nM, $m/z = 406.2$ $[M + H]^+$. 1H NMR (400 MHz, DMSO- d_6) δ 11.03 (br s, 1 H), 8.76 (d, 1 H, $J = 4.8$ Hz), 8.28 (d, 1 H, $J = 2.4$ Hz), 8.17 (d, 1 H, $J = 8.0$ Hz), 8.08 (ddd, 1 H, $J = 7.6, 7.6, 1.6$ Hz), 8.01 (dd, 1 H, $J = 8.8, 2.4$ Hz), 7.72–7.68 (m, 1 H), 7.52–7.30 (m, 6 H), 4.36 (dd, 1 H, $J = 9.6, 5.2$ Hz), 3.42 (dd, 1 H, $J = 18.4, 9.6$ Hz), 2.97 (dd, 1 H, $J = 18.4, 5.2$ Hz); ^{13}C NMR (125 MHz, DMSO- d_6 , mixture of diastereomers) δ 177.1, 175.4, 175.1, 163.3, 149.5, 148.7, 140.8, 140.7, 138.9, 138.5, 137.9, 131.8, 131.7, 131.2, 130.9, 129.3, 129.1, 128.7, 128.4, 127.9, 127.7, 126.0, 125.9, 123.2, 121.4, 121.3, 120.24, 120.15, 46.5, 46.2, 37.7, 37.5. HRMS calcd for $C_{22}H_{17}N_3O_3Cl$ $[M + H]^+$, 406.0958; found 406.0958.

■ ASSOCIATED CONTENT

Supporting Information

Experimental procedures, spectroscopic data, and NMR data for selected compounds and biological procedures. This material is available free of charge via the Internet at <http://pubs.acs.org>. VU0400195, **20f**, has been declared an MLPCN mGlu $_4$ probe (ML 182, CID 46869947, MLS 003171619) and is available from BioFocus, South San Francisco, CA.

■ AUTHOR INFORMATION

Corresponding Author

*For C.M.N.: phone, 615-343-4303; fax, 615-343-3088; e-mail, colleen.niswender@vanderbilt.edu. For C.R.H.: phone, 615-936-6892; fax, 615-936-4381; e-mail, corey.r.hopkins@vanderbilt.edu.

■ ACKNOWLEDGMENTS

The authors warmly acknowledge Emily L. Days, Tasha Nalywajko, Cheryl A. Austin, and Michael Baxter Williams for their critical contributions to the HTS portion of the project; Matt Mulder, Chris Denicola, Nathan Kett, and Sichen Chang for the purification of compounds utilizing the mass-directed HPLC system; and Katrina Brewer for technical assistance with the PK assays. The dog cassette in vivo experiment was performed at Calvert Labs, and the rhesus in vivo experiment was performed at the Yerkes Primate Center at Emory University, GA. This work was supported by the National Institute of Mental Health, National Institute of Neurological Disorders and Stroke, the Michael J. Fox Foundation, the Vanderbilt Department of Pharmacology, and the Vanderbilt Institute of Chemical Biology. In addition, the authors thank the NIH/MLPCN (Grant SU54MH084659-02) for support of this research. Vanderbilt is a member of the MLPCN and

houses the Vanderbilt Specialized Chemistry Center for Accelerated Probe Development.

■ ABBREVIATIONS USED

SAR, structure–activity relationship; mGluR, metabotropic glutamate receptor; PAM, positive allosteric modulator; HTS, high-throughput screening; CL_{int} , intrinsic clearance; PPB, plasma protein binding; AUC, area under the curve; GPCR, G-protein-coupled receptor; **1**, *N*-phenyl-7-(hydroxyimino)-cyclopropa[*b*]chromen-1a-carboxamide; CNS, central nervous system; PD, Parkinson's disease; GIRK, G-protein-coupled inwardly rectifying potassium channel; CYP, cytochrome P450; TPSA, topological polar surface area; CL_{HEP} , predicted hepatic clearance; *B/P*, brain/plasma ratio; CRC, concentration–response curve; *fu*, amount free and unbound (in %); DA, dopamine; PK, pharmacokinetics; BBB, blood–brain barrier; MW, molecular weight; FS, fold shift; RLM, rat liver microsome

■ REFERENCES

- (1) Dauer, W.; Przedborski, S. Parkinson's disease: mechanisms and models. *Neuron* **2003**, *39*, 889–909.
- (2) Schapira, A. H. V. Neurobiology and treatment of Parkinson's disease. *Trends Pharmacol. Sci.* **2009**, *30*, 41–47.
- (3) Hefti, F. F. Parkinson's Disease. *Drug Discovery Nerv. Syst. Dis.* **2005**, 183–204.
- (4) Fahn, S. Description of Parkinson's disease as a clinical syndrome. *Ann. N.Y. Acad. Sci.* **2003**, 991, 1–14.
- (5) Warner, T. T.; Schapira, A. H. V. Genetic and environmental factors in the cause of Parkinson's disease. *Ann. Neurol.* **2003**, *53*, S16–S25.
- (6) Jellinger, K. A. Recent developments in the pathology of Parkinson's disease. *J. Neural Transm.* **2002**, *62*, 347–376.
- (7) Parkinson, J. *An Essay on the Shaking Palsy*; London, Sherwood, Neely and Jones: London, 1817.
- (8) Fahn, S. The history of dopamine and levodopa in the treatment of Parkinson's disease. *Mov. Disord.* **2008**, *23*, S497–S508.
- (9) Baas, H.; Beiske, A. G.; Ghika, J.; Jackson, M.; Oertel, W. H.; Poewe, W.; Ransmayr, G. Catechol-*O*-methyltransferase inhibition with tolcapone reduces the “wearing off” phenomenon and levodopa requirements in fluctuating Parkinsonian patients. *Neurology* **1998**, *50*, S46–S53.
- (10) Stocchi, F. The levodopa wearing-off phenomenon in Parkinson's disease: pharmacokinetic considerations. *Exp. Opin. Pharmacother.* **2006**, *7*, 1399–1407.
- (11) Marek, K.; Jennings, D.; Seibyl, J. Do dopamine agonists or levodopa modify Parkinson's disease progression? *Eur. J. Neurol.* **2002**, *9*, 15–22.
- (12) Conn, P. J.; Battaglia, G.; Marino, M. J.; Nicoletti, F. Metabotropic glutamate receptors in the basal ganglia motor circuit. *Nat. Rev. Neurosci.* **2005**, *6*, 787–798.
- (13) Conn, P. J.; Pin, J.-P. Pharmacology and functions of metabotropic glutamate receptors. *Annu. Rev. Pharmacol. Toxicol.* **1997**, *37*, 205–237.
- (14) Conn, P. J.; Christopoulos, A.; Lindsley, C. W. Allosteric modulators of GPCRs: a novel approach for the treatment of CNS disorders. *Nat. Rev. Drug Discovery* **2009**, *8*, 41–54.
- (15) Cuomo, D.; Martella, G.; Barabino, E.; Platania, P.; Vita, D.; Madeo, G.; Selvam, C.; Goudet, C.; Oueslati, N.; Pin, J.-P.; Acher, F.; Pisani, A.; Beurrier, C.; Melon, C.; Kerkerian-LeGoff, L.; Gubellini, P. Metabotropic glutamate receptor subtype 4 selectively modulates both glutamate and GABA transmission in the striatum: implications for Parkinson's disease treatment. *J. Neurochem.* **2009**, *109*, 1096–1105.
- (16) Lindsley, C. W.; Niswender, C. M.; Engers, D. W.; Hopkins, C. R. Recent progress in the development of mGluR4 positive allosteric modulators for the treatment of Parkinson's disease. *Curr. Top. Med. Chem.* **2009**, *9*, 949–963.
- (17) Hopkins, C. R.; Lindsley, C. W.; Niswender, C. M. mGluR4 positive allosteric modulation as potential treatment of Parkinson's disease. *Future Med. Chem.* **2009**, *1*, 501–513.
- (18) Engers, D. W.; Niswender, C. M.; Weaver, C. D.; Jadhav, S.; Menon, U. N.; Zamorano, R.; Conn, P. J.; Lindsley, C. W.; Hopkins, C. R. Synthesis and evaluation of a series of heterobiaryl amides that are centrally penetrant metabotropic glutamate receptor 4 (mGluR4) positive allosteric modulators (PAMs). *J. Med. Chem.* **2009**, *52*, 4115–4118.
- (19) Engers, D. W.; Field, J. R.; Le, U.; Zhou, Y.; Bolinger, J. D.; Zamorano, R.; Blobaum, A. L.; Jones, C. K.; Jadhav, S.; Weaver, C. D.; Conn, P. J.; Lindsley, C. W.; Niswender, C. M.; Hopkins, C. R. Discovery, synthesis, and structure–activity relationship development of a series of *N*-(4-acetamido)phenylpicolinamides as positive allosteric modulators of metabotropic glutamate receptor 4 (mGlu₄) with CNS exposure in rats. *J. Med. Chem.* **2011**, *54*, 1106–1110.
- (20) East, S. P.; Bamford, S.; Dietz, M. G. A.; Eickmeier, C.; Flegg, A.; Feger, B.; Gemkow, M. J.; Heilker, R.; Hengerer, B.; Kotey, A.; Loke, P.; Schänzle, G.; Schubert, H.-D.; Scott, J.; Whittaker, M.; Williams, M.; Zawadzki, P.; Gerlach, K. An orally bioavailable positive allosteric modulator of the mGlu₄ receptor with efficacy in an animal model of motor dysfunction. *Bioorg. Med. Chem. Lett.* **2010**, *20*, 4901–4905.
- (21) Compounds **1** (PHCCC), **2** (VU0155041), and **3** (VU0361737) are now available from TOCRIS Bioscience (catalog nos. 1027, 3248, and 3707, respectively).
- (22) Hopkins, C. R.; Niswender, C. M.; Lewis, L. M.; Weaver, C. D.; Lindsley, C. W. “Discovery of a potent, selective and in vivo active mGluR4 positive allosteric modulator” **2011**, DOI: NBK50684. PMID: 21433377. <http://www.ncbi.nlm.nih.gov/pubmed/21433377>.
- (23) Niswender, C. M.; Lebois, E. P.; Luo, Q.; Kim, K.; Muchalski, H.; Yin, H.; Conn, P. J.; Lindsley, C. W. Positive allosteric modulators of the metabotropic glutamate receptor subtype 4 (mGluR4): Part I. Discovery of pyrazolo[3,4-*d*]pyrimidines as novel mGluR4 positive allosteric modulators. *Bioorg. Med. Chem. Lett.* **2008**, *18*, 5626–5630.
- (24) Williams, R.; Niswender, C. M.; Luo, Q.; Le, U.; Conn, P. J.; Lindsley, C. W. Positive allosteric modulators of the metabotropic glutamate receptor subtype 4 (mGluR4). Part II: Challenges in hit-to-lead. *Bioorg. Med. Chem. Lett.* **2009**, *19*, 962–966.
- (25) Engers, D. W.; Gentry, P. R.; Williams, R.; Bolinger, J. D.; Weaver, C. D.; Menon, U. N.; Conn, P. J.; Lindsley, C. W.; Niswender, C. M.; Hopkins, C. R. Synthesis and SAR of novel, 4-(phenylsulfamoyl)phenylacetamide mGlu₄ positive allosteric modulators (PAMs) identified by functional high-throughput screening (HTS). *Bioorg. Med. Chem. Lett.* **2010**, *20*, 5175–5178.
- (26) Niswender, C. M.; Johnson, K. A.; Luo, Q.; Ayala, J. E.; Kim, C.; Conn, P. J.; Weaver, C. D. A novel assay of G_{i/o}-linked G protein-coupled receptor coupling to potassium channels provides new insights into the pharmacology of the group III metabotropic glutamate receptors. *Mol. Pharmacol.* **2008**, *73*, 1213–1224.
- (27) Reynolds, I. J. Metabotropic Glutamate Receptors as Therapeutic Targets in Parkinson's Disease. Presented at the 6th International Meeting on Metabotropic Glutamate Receptors, Taormina, Sicily, Italy, September 14–19, 2008.
- (28) Slee, D. H.; Zhang, X.; Moorjani, M.; Lin, E.; Lanier, M. C.; Chen, Y.; Rueter, J. K.; Lechner, S. M.; Markison, S.; Malany, S.; Joswig, T.; Santos, M.; Gross, R. S.; Williams, J. P.; Castro-Palmino, J. C.; Cresp, M. I.; Prat, M.; Gual, S.; Díaz, J.-L.; Wen, J.; O'Brien, Z.; Saunders, J. Identification of novel, water-soluble, 2-amino-*N*-pyrimidin-4-yl acetamides as A_{2A} receptor antagonists with in vivo efficacy. *J. Med. Chem.* **2008**, *51*, 400–406.
- (29) VU0400195 (ML182) has been declared a probe via the Molecular Libraries Probe Production Centers Network (MLPCN) and is available through the network. See <http://mli.nih.gov/mli/>.